Colloids and Surfaces B: Biointerfaces 84 (2011) 484–490

Contents lists available at ScienceDirect

Colloids and Surfaces B: Biointerfaces

journal homepage: www.elsevier.com/locate/colsurfb

Preparation of surface plasmon resonance biosensor based on magnetic core/shell Fe_3O_4/SiO_2 and $Fe_3O_4/Ag/SiO_2$ nanoparticles

Liying Wang, Ying Sun, Jing Wang, Jian Wang, Aimin Yu, Hanqi Zhang, Daqian Song*

College of Chemistry, Jilin University, Qianjin Street 2699, Changchun 130012, PR China

ARTICLE INFO

Article history:
Received 1 September 2010
Received in revised form 4 January 2011
Accepted 1 February 2011
Available online 25 February 2011

Keywords:
Core/shell structure
Fe_3O_4/SiO_2 nanoparticles
$Fe_3O_4/Ag/SiO_2$ nanoparticles
Surface plasmon resonance

ABSTRACT

In this paper, surface plasmon resonance biosensors based on magnetic core/shell Fe_3O_4/SiO_2 and $Fe_3O_4/Ag/SiO_2$ nanoparticles were developed for immunoassay. With Fe_3O_4 and Fe_3O_4/Ag nanoparticles being used as seeding materials, Fe_3O_4/SiO_2 and $Fe_3O_4/Ag/SiO_2$ nanoparticles were formed by hydrolysis of tetraethyl orthosilicate. The aldehyde group functionalized magnetic nanoparticles provide organic functionality for bioconjugation. The products were characterized by scanning electronic microscopy (SEM), transmission electronic microscopy (TEM), FTIR and UV–vis absorption spectrometry. The magnetic nanoparticles possess the unique superparamagnetism property, exceptional optical properties and good compatibilities, and could be used as immobilization matrix for goat anti-rabbit IgG. The magnetic nanoparticles can be easily immobilized on the surface of SPR biosensor chip by a magnetic pillar. The effects of Fe_3O_4/SiO_2 and $Fe_3O_4/Ag/SiO_2$ nanoparticles on the sensitivity of SPR biosensors were also investigated. As a result, the SPR biosensors based on Fe_3O_4/SiO_2 nanoparticles and $Fe_3O_4/Ag/SiO_2$ nanoparticles exhibit a response for rabbit IgG in the concentration range of 1.25–20.00 $\mu g\,ml^{-1}$ and 0.30–20.00 $\mu g\,ml^{-1}$, respectively.

1. Introduction

Recently, magnetic nanoparticles as an immobilization matrix have been increasingly applied to immobilizing proteins, enzymes, and other bioactive agents in analytical biochemistry, medicine, and biotechnology [1]. In addition to their applications in the immobilization of biomolecules, magnetic nanoparticles have found many other applications such as bioseparation [2], drug delivery [3,4], biosensors [5], DNA detection [6], and molecular interactions in live cells [7]. Pure magnetic nanoparticles are likely to form a large aggregation, have fewer activating group and be easily oxidized or dissolved in an acid medium [8]. Therefore, a suitable coating on the surface of the pure magnetic nanoparticles is essential to avoid such limitations, meanwhile improves the physicochemical properties of the nanoparticles and maintains the colloidal suspension stability within the biological environment.

Coating biocompatible layers and incorporating optically active components onto magnetic nanoparticles surface have been widely studied [9–12]. Core–shell nanoparticles have attracted considerable attentions since the shells could offer protection to the cores and introduce new properties to the hybrid structures [13]. Core/shell $Fe_3O_4/Au/Ag$ nanoparticles have been synthesized and shown interesting optical properties in Au, Ag and magnetic properties in Fe_3O_4 [14]. Silica is an important shell-forming material owning to its high chemical and thermal stabilities, large surface areas and good compatibilities with other materials [15–17]. The silica-coated magnetic nanoparticles not only offer improved stability but also help in binding the various biological ligands at the nanoparticles surface [18,19].

Surface plasmon resonance (SPR) has been widely used as a powerful analytical technique for the study of biomolecular interactions [20]. Compared with other biosensor technologies, SPR biosensor have the advantages of label free detection, small sample volume and performed in real time. These characteristics make the SPR technique an easy, convenient and reliable one for studying the molecular recognition [21]. The SPR sensor chip surface is usually coated with sulfhydryl compounds to form a sensing layer on the metal film substrate [22]. Then the receptor molecules such as antibody could be covalently immobilized on the activated surface. Effective immobilization of biomolecules on the sensor surface is crucial in enhancing the sensitivity of SPR biosensor. Magnetic nanoparticles have increasingly been used in the area of bioscience recently [23,24]. The combined approach of magnetic nanoparticles and IR spectroscopy was used to detect complex food matrixes through spectroscopic fingerprinting and special selectivity due to antibody–antigen immunoreaction [25]. An impedance biosensor was constructed using interdigitated array microelectrode coupled with magnetic nanoparticle–antibody conjugates

* Corresponding author. Tel.: +86 431 85168399; fax: +86 431 85112355.
E-mail address: songdq@jlu.edu.cn (D. Song).

0927-7765/$ – see front matter © 2011 Elsevier B.V. All rights reserved.
doi:10.1016/j.colsurfb.2011.02.003

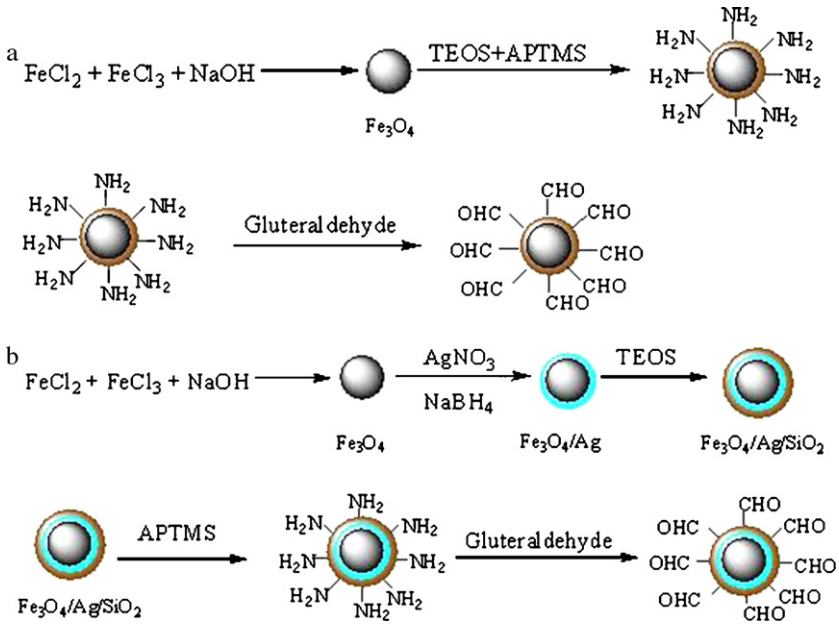

Fig. 1. Schematic illustration of the formation of Fe_3O_4/SiO_2 (a) and $Fe_3O_4/Ag/SiO_2$ (b) magnetic nanoparticles.

[26]. A glucose biosensor was prepared with Fe_3O_4 nanoparticles containing Prussian blue and glucose oxidase attracted to the surface of solid paraffin carbon paste electrode [27]. The SPR biosensor system with magnetic nanoparticles was also developed to detect the interaction between antibody and antigen [28–30]. Compared to traditional antibody immobilized on the sensing film, magnetic nanoparticles is a very promising choice for immobilization of antibody and there is no covalent link between the Au film and the antibody.

In this paper, core/shell Fe_3O_4/SiO_2 and $Fe_3O_4/Ag/SiO_2$ nanoparticles were synthesized and applied in the SPR biosensor. The aldehyde group functionalized Fe_3O_4/SiO_2 and $Fe_3O_4/Ag/SiO_2$ nanoparticles provide organic functionality for bioconjugation. Compared with traditional biosensor immobilized a self-assembled monolayer on the surface of the Au film, silica-coated magnetite nanoparticles have large surface areas and good compatibilities. So they are ideal immobilization matrixes for biomolecules and more beneficial to immobilization of antibody. Furthermore, because Ag nanoparticles could amplify the signal of the SPR biosensor, Fe_3O_4/Ag nanoparticles were prepared by reducing silver nitrate on the surface of Fe_3O_4 nanoparticles using the reverse micelle technology to enhance the sensitivity of the SPR biosensor [31]. Then silica was formed on the surface of Fe_3O_4/Ag nanoparticles by the hydrolysis and condensation of tetraethyl orthosilicate (TEOS) in the ethanol–ammonia mixture solution. Silica nanoparticles have been effectively applied to the immobilization of various biomolecules and proved to be excellent shell-forming material in the fabrication of biosensors. $Fe_3O_4/Ag/SiO_2$ nanoparticles have the characteristics of magnetic properties, good compatibilities and can enhance the sensitivity of the biosensor in a certain degree. The interactions of surface plasmon resonance of Au substrate and the localized surface plasmon resonance (LSPR) of the nanoparticles are expected to play crucial roles in the generation and manifestation of this enhancement. The core/shell Fe_3O_4/SiO_2 and $Fe_3O_4/Ag/SiO_2$ magnetic nanoparticles could be easily separated from liquid solution based on their superparamagnetic properties. When the aldehyde group functionalized magnetic nanoparticles were applied in SPR biosensor by a magnetic pillar, the gluteraldehyde was used as the bridge to bind the antibody and the magnetic nanoparticles. Then the antigen interacts with the antibody immobilized on the surface of the biosensor. The binding of protein–protein leads to changes in the refractive index at the sensor surface, which results in the shifts of resonant wavelength that can be easily measured by SPR biosensor.

2. Materials and methods

2.1. Reagents

Rabbit IgG, goat anti-rabbit IgG and human IgM were purchased from Beijing Boisynthesis Biotechnology Company. 3-Mercaptopropionic acid (MPA), 1-ethyl-3-(3-dimethylaminopropyl)carbodiimide (EDC) and *N*-hydroxysuccinimide (NHS) were purchased from Jkchemical. Ferric chloride hexahydrate ($FeCl_3{\cdot}6H_2O$), ferrous chloride tetrahydrate ($FeCl_2{\cdot}4H_2O$), sodium hydroxide, ammonia, tetraethyl orthosilicate (TEOS), 3-aminopropyltrimethoxysilane (APTMS), silver nitrate, gluteraldehyde, 2-propanol, Triton X-100, *n*-hexanol, cyclohexane, ethanol, cetyltrimethylammonium bromide (CTAB) and all other chemicals were of analytical reagent grade. All solutions were prepared with deionized water. Rabbit IgG, goat anti-rabbit IgG and human IgM were stored at −20 °C. Sodium phosphate buffered saline (PBS, 0.01 mol l^{-1}, pH 7.4) was used as running buffer.

2.2. Equipment

The wavelength modulation SPR biosensor installed in our laboratory was used [32]. It is working with Kretschmann configuration to achieve the resonant condition by attenuated total reflection (ATR) in a prism. A K9 glass slide was used and 2 nm adhesive layer of Cr followed by a 50 nm layer of Au was deposited on the glass slide. The glass slide with Au film was put on base of a prism (K9 glass) using a suitable index matching oil (cedar oil) to minimize reflective losses at the prism–substrate interface. A halogen tungsten lamp is used as the excitation light source in conjunction with a constant voltage transformer. A charge-coupled device (CCD) was used to collect the reflected light from the gold substrate. Magnetic pillar was immobilized under the optical prism.

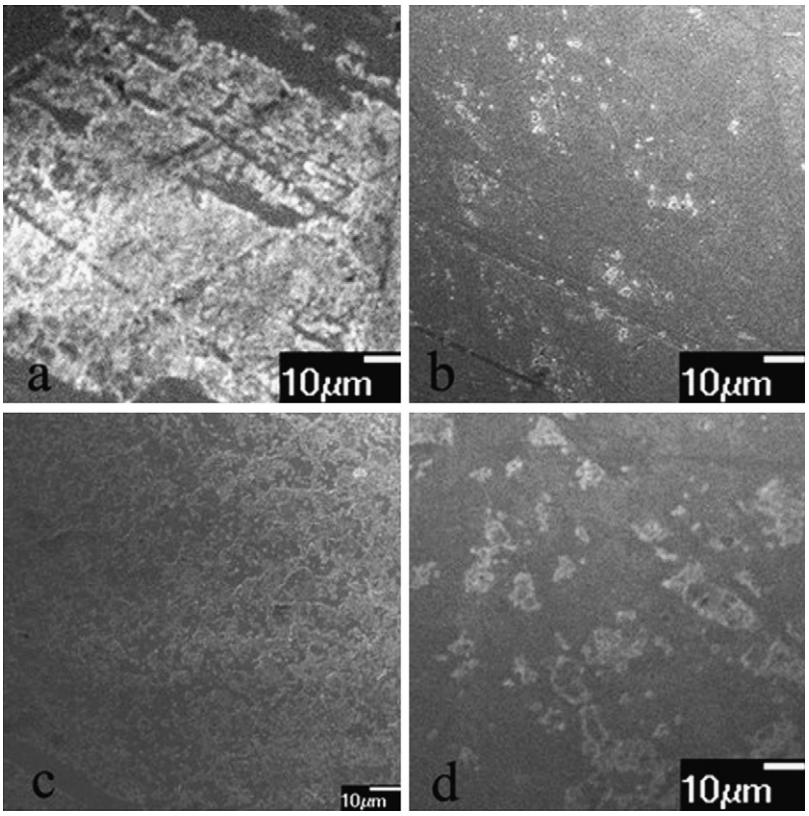

Fig. 2. SEM images of Fe_3O_4 nanoparticles (a), Fe_3O_4/SiO_2 nanoparticles (b), Fe_3O_4/Ag nanoparticles (c), and Fe_3O_4/Ag/SiO_2 nanoparticles (d).

The diameter and height of the magnetic pillar are 25 and 12 mm, respectively.

2.3. Procedures

2.3.1. Preparation of aldehyde group functionalized silica-coated magnetite nanoparticles

Amino group functionalized silica-coated magnetite nanoparticles were prepared according to the published procedure [33]. The Fe_3O_4 nanoparticles were prepared by chemical coprecipitation methods [34]. 2.6 g of $FeCl_3{\cdot}6H_2O$, 1.0 g of $FeCl_2{\cdot}4H_2O$ and 0.425 ml of HCl (12 mol l^{-1}) were dissolved in 12.5 ml deionized water to prepared a stock solution at first. Then the stock solution was added dropwise into 125 ml of NaOH (1.5 mol l^{-1}) solution under nitrogen gas protection and vigorous stirring at 80 °C. After the reaction, the obtained Fe_3O_4 nanoparticles were isolated from the solution using a permanent magnet and washed with deionized water four times. The precipitate was dispersed in 100 ml deionized water. The resulting in 0.724 ml of Fe_3O_4 magnetic nanoparticles solution obtained was diluted with 24 ml of water followed by the addition of 80 ml of 2-propanol, 20 ml of Triton X-100 and 2 ml of ammonia. Then 120 μl of TEOS and 30 μl of APTMS were added into the mixed solution under stirring for 3 h at room temperature. The magnetic nanoparticles were isolated from the mixture using a permanent magnet and washed with copious ethanol and water successively.

The amino group functionalized silica-coated magnetic nanoparticles were immersed in 1.25% glutaraldehyde aqueous solutions at room temperature under stirring for 1 h. Then, the modified magnetic nanoparticles were isolated using a permanent magnetic field and washed with water. These nanoparticles were dispersed in water and stored in 4 °C. The schematic illustration of the preparation of Fe_3O_4/SiO_2 magnetic nanoparticles is shown in Fig. 1(a).

2.3.2. Preparation of aldehyde group functionalized Fe_3O_4/Ag/SiO_2 nanoparticles

Fe_3O_4/Ag nanoparticles were synthesized by the reverse micelle technology [31]. 0.4 ml of Fe_3O_4 nanoparticles solution obtained was mixed with 7.0 ml of Triton X-100, 7.0 ml of *n*-hexanol and 37.5 ml of cyclohexane under vigorous stirring. Then, 1 ml of 0.10 mol l^{-1} $AgNO_3$ was added. After 30 min, 1 ml of 0.20 mol l^{-1} $NaBH_4$ was added into the solution. The mixture was stirred at room temperature for 4 h. After the reaction, the black Fe_3O_4/Ag nanoparticles were precipitated by adding excess acetone, and then isolated from the mixture using a permanent magnet. The precipitate was washed with ethanol and deionized water and then dispersed in 20 ml deionized water.

0.0145 g CTAB was added into the obtained Fe_3O_4/Ag nanoparticles solution under vigorous stirring. Subsequently, 5 ml of ethanol and 100 μl of TEOS were added into the above solution successively. The solution was stirred at room temperature for 3 h. After the reaction, the obtained Fe_3O_4/Ag/SiO_2 magnetite nanoparticles were isolated using a permanent magnet and dispersed in 30 ml of ethanol. Then 1 ml of ammonia and 100 μl of APTMS were added into the obtained Fe_3O_4/Ag/SiO_2 magnetite nanoparticles solution under vigorous stirring for 5 h at room temperature. The nanoparticles modified with amino group were isolated from the mixture using a permanent magnet and washed with copious ethanol and water successively. The procedure of Fe_3O_4/Ag/SiO_2 nanoparticles modified with aldehyde group was the same as the procedure mentioned above. The prepared magnetic nanoparticles were dispersed in water and stored at −4 °C when they were not used. The schematic illustration of the preparation of Fe_3O_4/Ag/SiO_2 magnetic nanoparticles is shown in Fig. 1(b).

2.3.3. Characterizations of the magnetic nanoparticles

The morphologies of Fe_3O_4, Fe_3O_4/SiO_2, Fe_3O_4/Ag and Fe_3O_4/Ag/SiO_2 nanoparticles were characterized by scanning elec-

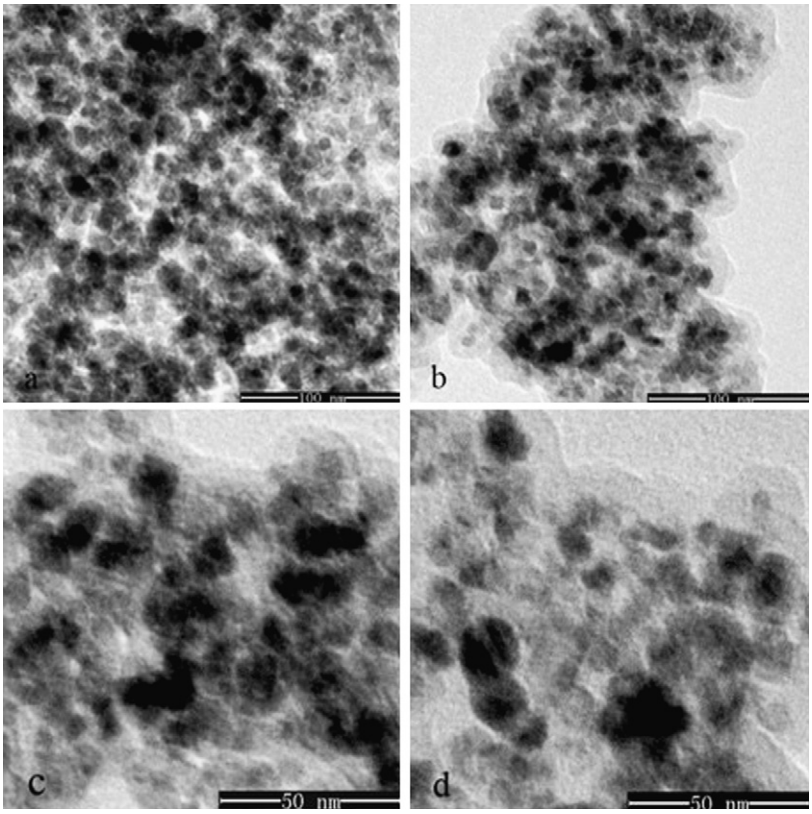

Fig. 3. TEM images of Fe_3O_4 nanoparticles (a), Fe_3O_4/SiO_2 nanoparticles (b), Fe_3O_4/Ag nanoparticles (c), and $Fe_3O_4/Ag/SiO_2$ nanoparticles (d).

tronic microscopy (SEM) and transmission electronic microscopy (TEM). The samples for SEM were obtained by immersing the Au film into the sample solutions, which a magnetic pillar was under for and then washing the Au film with water. The samples for TEM were obtained by placing drops of each sample on a copper grid. To confirm the structure of the magnetic nanoparticles, FTIR spectra were recorded of samples in the 500–4000 cm^{-1} region. The magnetic nanoparticles were isolated from the solution using a permanent magnet and then dried. The KBr compressed pellet method was adopted for solid samples. The UV–vis absorption spectra of the dispersions were measured by a UV–vis spectrometer. The samples were diluted with deionized water and ultrasonic treatment to make them homogeneously disperse in the solution before they were measured.

2.3.4. Preparation of SPR biosensors based on the modified magnetic nanoparticles

The glass slide with gold film was fixed to the flow cell on a prism. Deionized water was first injected into the flow cell. Then PBS was injected into the flow cell as the baseline solution. The aldehyde group functionalized Fe_3O_4/SiO_2 and $Fe_3O_4/Ag/SiO_2$ nanoparticles were isolated using a permanent magnet and redispersed in PBS buffer solution as they were used. After ultrasonic treatment, the modified magnetic nanoparticles homogeneously dispersed in the solution and then introduced into the flow cell equipped with a magnetic pillar under the prism for 5 h. The modified magnetic nanoparticles can be immobilized on the Au film by the magnetic pillar. After the modified magnetic nanoparticles were immobilized on the Au film, 100 $\mu g\,ml^{-1}$ goat anti-rabbit IgG solution was injected into the flow cell to covalently attach to the aldehyde-activated surfaces. After 12 h, PBS buffer was injected into the flow cell to wash off non-covalently bound antibody and to stabilize the baseline. PBS buffer is generally used as a solvent and plays a role in dissolving and protecting the reagents. PBS buffer could maintain the solution at a certain pH and a certain ions concentration, and keep the activity of the antibodies. Prior to the analysis, 1 $mol\,l^{-1}$ ethanolamine hydrochloride (pH 8.0) was used to block the non-specific binding sites on the biosensor surface for 10 min. The magnetic pillar was immobilized under the prism on the whole experiment process.

For comparison, the MPA self-assemble monolayer (SAM) was also constructed. PBS buffer was used as the baseline solution, and 10 $mmol\,l^{-1}$ MPA was injected into the flow cell. After 2 h, carboxyl group of MPA was activated with NHS under the catalysis of EDC for 20 min. Then 100 $\mu g\,ml^{-1}$ goat anti-rabbit IgG solution was injected. The next procedures were the same as those mentioned above.

2.3.5. Immunoassay

At room temperature, different concentrations of rabbit IgG diluted with PBS buffer were separately injected into the flow cell. The interaction between rabbit IgG in the solution and the goat anti-rabbit IgG immobilized on the SPR biosensor surface causes a change in the refractive index that is observed as the shift of the SPR resonant wavelength. Then PBS buffer was injected into the flow cell. When the antigen was dissociated from the antibody immobilized on biosensor surface, another sample was injected into the flow cell.

Traditionally, chemical reagents such as acid, base, or salt with high ion strength could be used to desorb antigens bound on a sensor surface. However, strong acid or base solution would destroy the activity of protein. Using of PBS buffer could overcome the problem. Due to a large amount of ions in the PBS buffer, the antigen could be washed by impulsive injection of PBS buffer [35]. When the concentration of rabbit IgG is low, the antigen is easy to be removed. When the concentration is too high, the antigen cannot

be removed completely. When the rabbit IgG was detected from low concentration to high concentration, it has little effect on the experimental results.

To examine the reliability of the assay, all determinations of the experiments were conducted three times.

To evaluate the selective binding of rabbit IgG, human IgM and BSA were determined by the same procedure.

3. Results and discussion

3.1. Preparation and characterization of magnetic nanoparticles

Fe_3O_4 nanoparticles were synthesized by co-precipitation of aqueous Fe^{2+}/Fe^{3+} salt solutions with the addition of a base. The morphologies of magnetite nanoparticles were characterized by SEM and TEM. Fig. 2 provides the SEM images of the prepared Fe_3O_4, Fe_3O_4/SiO_2, Fe_3O_4/Ag and $Fe_3O_4/Ag/SiO_2$ nanoparticles. Fig. 2(a) shows the SEM image of Fe_3O_4 nanoparticles and it can be seen that the nanoparticles were aggregative. Fig. 2(b)–(d) shows the SEM images of Fe_3O_4/SiO_2, Fe_3O_4/Ag and $Fe_3O_4/Ag/SiO_2$ nanoparticles, respectively. It can be seen that the aggregation of the modified magnetic nanoparticles was reduced significantly. Fig. 3 provides the TEM images of the prepared Fe_3O_4, Fe_3O_4/SiO_2, Fe_3O_4/Ag, and $Fe_3O_4/Ag/SiO_2$ nanoparticles. Fig. 3(a) and (c) shows the TEM image of Fe_3O_4 and Fe_3O_4/Ag nanoparticles and the average particle sizes are about 10 nm and 13 nm, respectively. Fig. 3(b) and (d) shows the TEM image of Fe_3O_4/SiO_2 and $Fe_3O_4/Ag/SiO_2$ nanoparticles and the average particle sizes are about 16 nm and 19 nm, respectively. Here the core–shell structures of Fe_3O_4/SiO_2 and $Fe_3O_4/Ag/SiO_2$ nanoparticles are shown. The experimental results showed that the surfaces of Fe_3O_4 and Fe_3O_4/Ag nanoparticles were fully covered with SiO_2 shell, and the thickness of layers were about 6 nm. Fe_3O_4 and Fe_3O_4/Ag nanoparticles are shown as dark dot and covered with an asymmetric SiO_2 shell.

3.2. Optical properties of magnetite nanoparticles

The magnetic nanoparticles were characterized by FTIR spectrum and UV–vis absorption spectrometry. The FTIR spectra of Fe_3O_4 nanoparticles, Fe_3O_4/SiO_2 nanoparticles and $Fe_3O_4/Ag/SiO_2$ nanoparticles are shown in Fig. 4. FTIR is an appropriate technique to study the chemical adsorption or chemical interaction. For the Fe_3O_4 nanoparticles, the characteristic absorption peak at 590 cm^{-1} is attributed to the Fe–O structure [36]. After SiO_2 is coated on the surface of Fe_3O_4 nanoparticles, the characteristic absorption peak at 1095 cm^{-1} is attributed to the Si–O–Si structure [9]. These absorption wavenumbers indicated that SiO_2 was successfully covered onto the surface of the Fe_3O_4 nanoparticles and the Fe_3O_4/Ag nanoparticles.

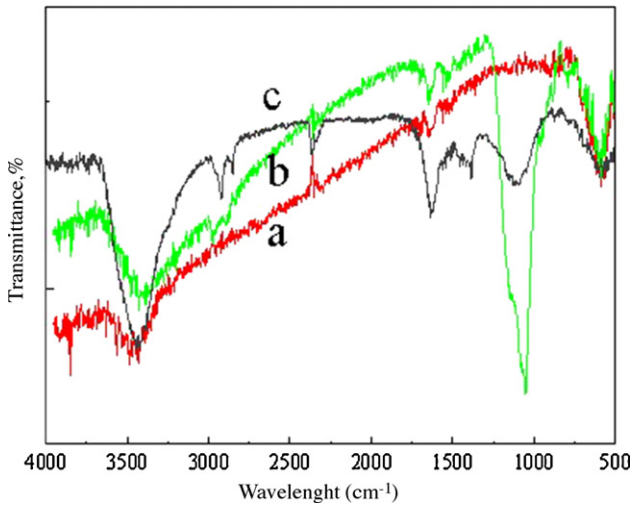

Fig. 4. FTIR spectra of Fe_3O_4 nanoparticles (a), Fe_3O_4/SiO_2 nanoparticles (b), and $Fe_3O_4/Ag/SiO_2$ nanoparticles (c).

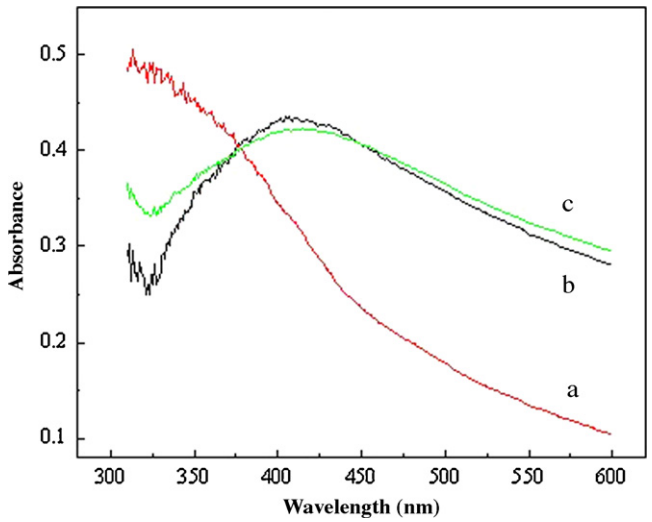

Fig. 5. UV–visible absorption spectra of Fe_3O_4 nanoparticles (a), Fe_3O_4/Ag nanoparticles (b), and $Fe_3O_4/Ag/SiO_2$ nanoparticles (c).

The UV–vis absorption spectra of the magnetic Fe_3O_4 nanoparticles, Fe_3O_4/Ag nanoparticles and $Fe_3O_4/Ag/SiO_2$ nanoparticles are shown in Fig. 5. The absorption intensity of Fe_3O_4 spectrum decreases with the increase of the wavelength in the range 320–600 nm and no obvious absorption peak is observed. When silver was deposited on the surface of Fe_3O_4 nanoparticle, the absorption peak maximum at around 400 nm, which is the characteristic of Ag nanoparticles, appears [37]. This result confirms the deposition of silver on the surface of Fe_3O_4 nanoparticles. After SiO_2 is coated on the surface of Fe_3O_4/Ag nanoparticles, the red shifts of the peak for Ag nanoparticles are observed. The peak maximum is centered at 414 nm. The silica shell also affects the width of peak, which is due to the confinement of the free electrons with the metal core in the case of smaller particles. All these effects suggest that the $Fe_3O_4/Ag/SiO_2$ nanoparticles have been formed.

The magnetic nanoparticles were repeatedly prepared several times and the optical properties of the magnetite nanoparticles are almost the same. So the reproducibility for preparing methods of the magnetite nanoparticles is satisfactory.

3.3. Preparation of SPR biosensors based on magnetic nanoparticles

Here, two types of SPR biosensors based on Fe_3O_4/SiO_2 nanoparticles and $Fe_3O_4/Ag/SiO_2$ nanoparticles were prepared. The glass slide with gold film connected to the prism with cedar oil, PBS buffer solution was injected into the flow cell as the baseline solution. Then the modified Fe_3O_4/SiO_2 nanoparticles and $Fe_3O_4/Ag/SiO_2$ nanoparticles solutions were separately introduced into the flow cell for preparation of the two types of biosensor. The shifts of the resonant wavelength due to the modified magnetic nanoparticles immobilized on the Au film were monitored in real time. Because of the magnetic pillar under the prism, the modified magnetic nanoparticles can be immobilized on the Au film easily. The maximum shifts of the resonant wavelength caused by forming this sensing layer is 5.12 nm for Fe_3O_4/SiO_2 nanoparticles and 7.12 nm for $Fe_3O_4/Ag/SiO_2$ nanoparticles. These indicated that the immobilizations on the sensor films were formed. The immobilization of

the magnetic nanoparticles on the Au film leads to changes in the refractive index at the sensor surface, which results in the shifts of resonant wavelength. The biosensor based on Fe_3O_4/SiO_2 nanoparticles has two advantages compared with traditional biosensor. First, the magnetic nanoparticles can be immobilized on the Au film easily, which greatly simplifies the operation. Second, in contrast to traditional biosensor contained only one layer of receptor molecules on the surface of the gold film, the modified magnetic nanoparticles have larger surface areas, better compatibilities and more numbers of receptor molecules, which are more beneficial for the immobilization of antibody. In addition to the above advantages, the biosensor based on $Fe_3O_4/Ag/SiO_2$ nanoparticles has another advantage. Ag nanoparticles could be used to amplify the signal of the SPR biosensor. The $Fe_3O_4/Ag/SiO_2$ magnetic nanoparticles not only help in binding the biomolecules at the nanoparticle surface but also offer high sensitivity.

3.4. Immobilization of goat anti-rabbit IgG

The SPR sensor chip surface is usually coated with sulfhydryl compounds to form a sensing layer on the metal film substrate. Then the antibody could be covalently immobilized on the activated surface. Here instead of functional with many different kinds of reagents as the link, the antibody could be immobilized on the Au film by magnetic nanoparticles. After the modified magnetic nanoparticles were immobilized on the Au film, goat anti-rabbit IgG at the concentration of 100 $\mu g\,ml^{-1}$ was injected into the flow cell to perform its binding on the activated surface. Due to the magnetic nanoparticles covered with aldehyde group, the antibody was structured on the gold surface strongly. The terminal aldehyde group can be bound with the amine group of the antibody to form Schiff bases easily. The activated biosensor surface effectively connected with antibody through covalent attachment. The kinetic adsorption curves of goat anti-rabbit IgG on the sensor surface are shown in Fig. 6. After 12 h, PBS buffer was injected into the flow cell. Then, 1 $mol\,l^{-1}$ ethanolamine hydrochloride (pH 8.0) was used to block the non-specific binding sites on the biosensor surface.

Fig. 6(a) shows the kinetic adsorption curves of goat anti-rabbit IgG on the biosensor based on MPA-SAM layer. Fig. 6(b) and (c) shows the kinetic adsorption curves of goat anti-rabbit IgG on the sensor based on Fe_3O_4/SiO_2 and $Fe_3O_4/Ag/SiO_2$ nanoparticles, respectively. It can be seen that the resonant wavelengths show

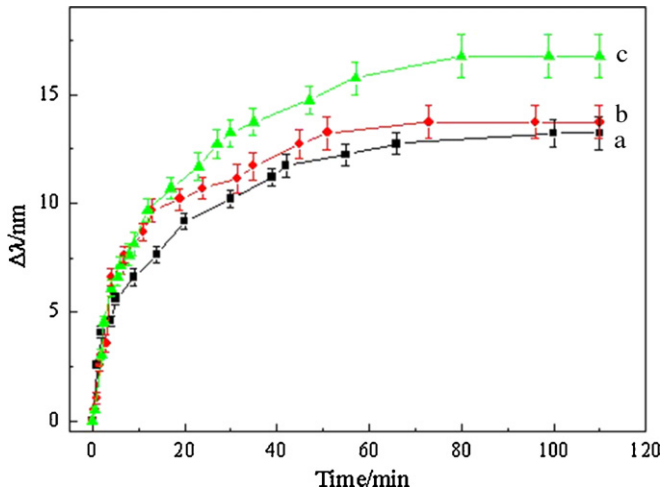

Fig. 6. Kinetic adsorption curves of goat anti-rabbit IgG at the concentration of 100 $\mu g\,ml^{-1}$. (a) The sensor based on MPA-SAM layer, (b) the sensor based on Fe_3O_4/SiO_2 nanoparticles, and (c) the sensor based on $Fe_3O_4/Ag/SiO_2$ nanoparticles.

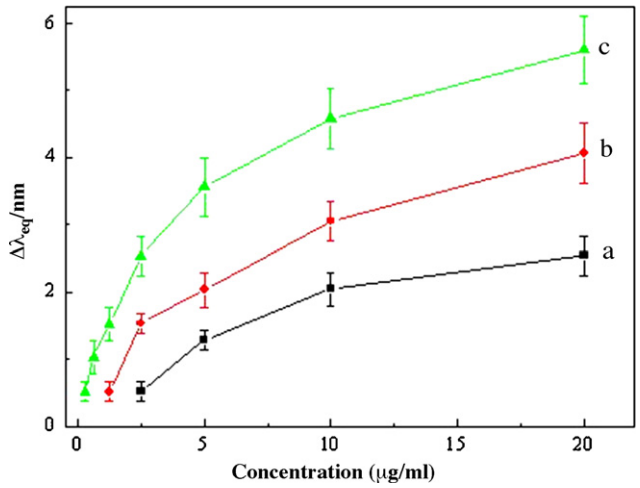

Fig. 7. The relationship between the concentration of rabbit IgG and the shifts in the resonant wavelength. (a) The sensor based on MPA-SAM layer, (b) the sensor based on Fe_3O_4/SiO_2 nanoparticles, and (c) the sensor based on $Fe_3O_4/Ag/SiO_2$ nanoparticles.

evident shift at first and then change slowly with the time increasing. The results indicated that the terminal aldehyde group of gluteraldehyde has a strong response to antibody and the antibody could be immobilized steadily on the biosensor surface. The covalent attachment between the amine group and the aldehyde group is a good stratagem for the immobilization of antibody. It can be seen from Fig. 6 that the maximum resonant wavelength shift for immobilization of goat anti-rabbit IgG on the surface of MPA, Fe_3O_4/SiO_2 and $Fe_3O_4/Ag/SiO_2$ nanoparticles are 13.22, 13.73 nm and 16.77 nm, respectively. After 12 h, the maximum resonant wavelength shift for immobilization of goat anti-rabbit IgG on the surface of MPA, Fe_3O_4/SiO_2 and $Fe_3O_4/Ag/SiO_2$ nanoparticles are 16.78 nm, 17.80 nm and 21.45 nm, respectively. After PBS buffer was injected into the flow cell, the maximum resonant wavelength shift for immobilization of goat anti-rabbit IgG on the surface of MPA, Fe_3O_4/SiO_2 and $Fe_3O_4/Ag/SiO_2$ nanoparticles are 15.25 nm, 16.78 nm and 20.43 nm, respectively. Due to a large amount of ions in the PBS buffer, PBS buffer could be used to wash the non-specific binding of antibodies on the sensor surface. When PBS was continuously injected into the flow cell, for a certain time, the non-specific binding of antibodies will be washed [35]. Compared with the biosensors based on MPA-SAM layer and Fe_3O_4/SiO_2 nanoparticles, when the biosensor based on $Fe_3O_4/Ag/SiO_2$ nanoparticles was used, the maximum resonant wavelength shift has a modest increase.

3.5. Determination of rabbit IgG

At room temperature, after goat anti-rabbit IgG was immobilized on the biosensor surface, rabbit IgG at different concentrations was separately injected into the flow cell. The shifts of resonant wavelength due to antibody–antigen immunoreaction were measured. The SPR response of rabbit IgG adsorption can be monitored in real time. Fig. 7 shows the relationship between the shifts in the resonant wavelength and the concentrations of rabbit IgG. It can be seen that the SPR biosensor based on MPA-SAM layer shows a response to rabbit IgG in the concentration range of 2.50–20.00 $\mu g\,ml^{-1}$. The minimum shift of resonant wavelength is 0.51 nm at 2.50 $\mu g\,ml^{-1}$ and the maximum shift of resonant wavelength is 2.54 nm at 20.00 $\mu g\,ml^{-1}$. The SPR biosensor based on Fe_3O_4/SiO_2 nanoparticles shows a response to rabbit IgG in the concentration range of 1.25–20.00 $\mu g\,ml^{-1}$. The minimum shift of resonant wavelength is 0.51 nm at 1.25 $\mu g\,ml^{-1}$ and the maximum

shift of resonant wavelength is 4.06 nm at 20.00 μg ml^{-1}. The SPR biosensor based on Fe_3O_4/Ag/SiO_2 nanoparticles shows a response to rabbit IgG in the concentration range of 0.30–20.00 μg ml^{-1}. The minimum shift of resonant wavelength is 0.51 nm at 0.30 μg ml^{-1} and the maximum shift of resonant wavelength is 5.60 nm at 20.00 μg ml^{-1}.

The detection of molecular interactions on a functionalized surface is achieved by monitoring the changes of the film thickness and the refractive index due to biomolecular binding. When Fe_3O_4/SiO_2 and Fe_3O_4/Ag/SiO_2 nanoparticles were applied in the SPR biosensor, the thickness of the sensing membrane increased and the resonant wavelength moved to longer wavelength. In Fe_3O_4/Ag/SiO_2 nanoparticles, the interaction between the LSPR of the Ag with the propagating plasmon in the Au film might lead to large changes in SPR reflectivity through strong optical coupling between the film and particle, which further enhanced the shift of resonant wavelength. These two factors result in the sensitivity enhancement of the wavelength-modulation SPR biosensor. The proposed biosensors extended the application of magnetic nanoparticles in immunoassay.

The evaluation of the non-specific binding interaction was performed by detecting human IgM and BSA. After the goat anti-rabbit IgG was immobilized on the surface of the biosensor, human IgM and BSA at the concentration of 10 μg ml^{-1} were separately injected into the flow cell for 30 min. There were no observable shifts of the resonant wavelength, which indicated the selective binding of rabbit IgG.

4. Conclusion

The detection of rabbit IgG with the wavelength modulation SPR biosensors based on aldehyde group functionalized Fe_3O_4/SiO_2 and Fe_3O_4/Ag/SiO_2 magnetic nanoparticles were presented. The shapes and the average sizes of the magnetic nanoparticles were measured by SEM and TEM. The magnetic nanoparticles could be immobilized on the surface of SPR biosensor chip by a magnetic pillar and then offer the opportunities for effectively connect with antibody. The biosensor based on Fe_3O_4/SiO_2 nanoparticles exhibits a response in the concentration range of 1.25–20.00 μg ml^{-1} and the biosensor based on Fe_3O_4/Ag/SiO_2 nanoparticles exhibits a response in the concentration range of 0.30–20.00 μg ml^{-1}.

Acknowledgements

This work was supported by National Natural Science Foundation of China (No. 20727003, 21075049) and Science and Technology Developing Foundation of Jilin Province (No. 20070551, 20100356).

References

[1] G.K. Kouassi, J. Irudayaraj, Anal. Chem. 78 (2006) 3234–3241.
[2] A. Ito, M. Shinkai, H. Honda, T. Kobayashi, J. Biosci. Bioeng. 100 (2005) 1–11.
[3] S.H. Hu, C.H. Tsai, C.F. Liao, D.M. Liu, S.Y. Chen, Langmuir 24 (2008) 11811–11818.
[4] A. Lübbe, C. Bergemann, J. Brock, D.G. McClure, J. Magn. Magn. Mater. 194 (1999) 149–155.
[5] S.G. Grancharov, H. Zeng, S. Sun, S.X. Wang, S. O'Brien, C.B. Murray, J.R. Kirtley, G.A. Held, J. Phys. Chem. B 109 (2005) 13030–13035.
[6] Y. Weizmann, F. Patolsky, E. Katz, I. Willner, J. Am. Chem. Soc. 125 (2003) 3452–3454.
[7] Y.M. Huh, Y.W. Jun, H.T. Song, S.J. Kim, J.S. Choi, J.H. Lee, S. Yoon, K.S. Kim, J.S. Shin, J.S. Suh, J. Cheon, J. Am. Chem. Soc. 127 (2005) 12387–12391.
[8] H.H. Yang, S.Q. Zhang, X.L. Chen, Z.X. Zhuang, J.G. Xu, X.R. Wang, Anal. Chem. 76 (2004) 1316–1321.
[9] Y.H. Lien, T.M. Wu, J. Colloid Interface Sci. 326 (2008) 517–521.
[10] A.P. Philipse, M.P.B. van Bruggen, C. Pathmamanoharan, Langmuir 10 (1994) 92–99.
[11] C.S. Levin, C. Hofmann, T.A. Ali, A.T. Kelly, E. Morosan, P. Nordlander, K.H. Whitmire, N.J. Halas, ACS Nano 3 (2009) 1379–1388.
[12] L. Wang, J. Luo, Q. Fan, M. Suzuki, I.S. Suzuki, M.H. Engelhard, Y. Lin, N. Kim, J.Q. Wang, C.J. Zhong, J. Phys. Chem. B 109 (2005) 21593–21601.
[13] L.M. Liz-Marzán, M. Giersig, P. Mulvaney, Langmuir 12 (1996) 4329–4335.
[14] Z.C. Xu, Y.L. Hou, S.H. Sun, J. Am. Chem. Soc. 129 (2007) 8698–8699.
[15] Z.Y. Lu, J. Dai, X.N. Song, G. Wang, W.S. Yang, Colloid Surf. A 317 (2008) 450–456.
[16] Z.C. Zhang, L.M. Zhang, L. Chen, L.G. Chen, Q.H. Wan, Biotechnol. Prog. 22 (2006) 514–518.
[17] X.L. Zhao, Y. Shi, T. Wang, Y.Q. Cai, G.B. Jiang, J. Chromatogr. A 1188 (2008) 140–147.
[18] C. Grüttner, S. Rudershausen, J. Magn. Magn. Mater. 225 (2001) 1–7.
[19] T.T. Baby, S. Ramaprabhu, Talanta 80 (2010) 2016–2022.
[20] J. Homola, S.S. Yee, G. Gauglitz, Sens. Actuators B 54 (1999) 3–15.
[21] X. Liu, D.Q. Song, Q.L. Zhang, Y. Tian, L. Ding, H.Q. Zhang, Trend Anal. Chem. 24 (2005) 887–983.
[22] L.Y. Wang, Y. Sun, J. Wang, X.N. Zhu, F. Jia, Y.B. Cao, X.H. Wang, H.Q. Zhang, D.Q. Song, Talanta 78 (2009) 265–269.
[23] M.A.M. Gijs, F. Lacharme, U. Lehmann, Chem. Rev. 110 (2010) 1518–1563.
[24] A.P. Fan, C. Lau, J.Z. Lu, Anal. Chem. 77 (2005) 3238–3242.
[25] S.P. Ravindranath, L.J. Mauer, C. Deb-Roy, J. Irudayaraj, Anal. Chem. 81 (2009) 2840–2846.
[26] M. Varshney, Y. Li, Biosens. Bioelectron. 22 (2007) 2408–2414.
[27] J.P. Li, X.P. Wei, Y.H. Yuan, Sens. Actuators B 139 (2009) 400–406.
[28] Y. Sun, Y.P. Bai, D.Q. Song, X.Z. Li, L.Y. Wang, H.Q. Zhang, Biosens. Bioelectron. 23 (2007) 473–478.
[29] S.D. Soelberg, R.C. Stevens, A.P. Limaye, C.E. Furlong, Anal. Chem. 81 (2009) 2357–2363.
[30] J. Wang, Y. Sun, L.Y. Wang, X.N. Zhu, H.Q. Zhang, D.Q. Song, Colloid Surf. B 81 (2010) 600–606.
[31] P. Gong, H.M. Li, X.X. He1, K.M. Wang, J.B. Hu, W.H. Tan, S.C. Zhang, X.H. Yang, Nanotechnology 18 (2007) 285604 (pp. 7).
[32] L.Y. Wang, J. Wang, S.L. Zhang, Y. Sun, X.N. Zhu, Y.B. Cao, X.H. Wang, H.Q. Zhang, D.Q. Song, Anal. Chim. Acta 653 (2009) 109–115.
[33] J.L. Gong, Y. Liang, Y. Huang, J.W. Chen, J.H. Jiang, G.L. Shen, R.Q. Yu, Biosens. Bioelectron. 22 (2007) 1501–1507.
[34] X.L. Zhao, Y.Q. Cai, T. Wang, Y.L. Shi, G.B. Jiang, Anal. Chem. 80 (2008) 9091–9096.
[35] R. Pei, X. Cui, X. Yang, E. Wang, Talanta 53 (2000) 481–488.
[36] J.L. Zhang, R.S. Srivastava, R.D.K. Misra, Langmuir 23 (2007) 6342–6351.
[37] K. Xu, J.X. Wang, X.L. Kang, J.F. Chen, Mater. Lett. 63 (2009) 31–33.